

SUMO1-modified DNA methyltransferase 1 induces DNA hypermethylation of VWC2 in the development of colorectal cancer

Xiao-Hu CHENG*, Tong-Tong XU*, Lian-Bang ZHOU, Fang-Yuan LI, Song WANG, Huan-Ru LIANG, Jing-Jing TANG, Chang-Qin DUAN, Heng JIANG, Ying-Feng ZHANG, Zhi-Ning LIU*

Department of General Surgery, The Second Hospital of Anhui Medical University, Hefei, Anhui, China

*Correspondence: liuzl_gs10142@163.com

*Contributed equally to this work.

Received August 17, 2022 / Accepted November 2, 2022

Aberrant DNA methylation of genes is closely linked to many aspects of tumor development. This study focuses on the effect of DNA hypermethylation of von Willebrand factor C domain containing 2 (VWC2) on colorectal cancer (CRC) progression and the underpinning mechanism. According to data in the bioinformatic systems, VWC2 had the highest degree of DNA methylation in colonic adenocarcinoma, and it showed DNA hypermethylation in rectal adenocarcinoma as well. CRC and the para-tumorous tissues were collected from 86 patients. VWC2 was expressed at low levels in CRC samples and inversely correlated with tumor stage and tumor biomarker expression. DNA hypermethylation and reduced expression of VWC2 were also detected in CRC cell lines HCT-116 and HT29. VWC2 overexpression suppressed the malignant growth of cells *in vitro* and *in vivo*. Co-immunoprecipitation and western blot assays showed that small ubiquitin-like modifier 1 (SUMO1) mediated SUMOylation of DNA methyltransferase 1 (DNMT1) and strengthened its protein stability, which promoted DNA methylation and suppression of the VWC2 gene. In summary, this study demonstrates that SUMO1-mediated activation of DNMT1 induces DNA methylation and downregulation of VWC2 in CRC to augment cancer development.

Key words: SUMO1, DNMT1, VWC2, DNA methylation, colorectal cancer

Colorectal cancer (CRC) represents one of the most common neoplasms making up for approximately 10% of all cancer incidence and mortality rates across the globe [1, 2]. While surgical resection is a curable strategy for early-stage CRC, effective therapeutic options for patients with metastatic disease (25% of all diagnosed cases) are lacking [3]. Correspondingly, the survival rate of patients largely depends on the disease stage. The 5-year survival rate ranges from approximately 90% for stage I disease to slightly over 10% for stage IV disease [4, 5]. Although great progress has been made in CRC treatments, such as surgery, chemotherapy, radiotherapy, immunotherapy, and anti-epithelial growth factor receptor therapy, the prognosis of patients remains poor [6]. It is urgent to identify more oncogenic events implicated in the onset and progression of CRC.

CRC has a strong epigenetic component, and the epigenetic alterations act even prior to genetic changes in inducing malignant transformation of cancer cells [7]. DNA methylation represents one of the major epigenetic mechanisms by which cells use to manipulate gene expression, generally inducing transcriptional suppression and gene downregu-

lation [8]. There are three common DNA methyltransferases (DNMTs), DNMT1, DNMT3a, and DNMT3b, which catalyze the addition of methyl to cytosine residues at carbon 5 to induce DNA hypermethylation [9]. The DNA hypermethylation of tumor inhibitor genes is frequently involved in tumor initiation and development [10, 11]. Importantly, DNA methylation is a dynamic and reversible process, leaving the methylation modifications as potential targets for treatment [12]. Here, we obtained via bioinformatics tools that von Willebrand factor C domain containing 2 (VWC2) had a high DNA methylation level in CRC. VWC2 was found as an antagonist of bone morphogenetic proteins potentially linking to bone formation [13]. However, little is known about its role in tumor development.

SUMOylation represents one of the essential components of the ubiquitination proteasome system exerting critical functions in the maintenance of protein homeostasis and signal transduction, whose perturbation is linked to tumorigenesis [14]. The SUMOylation participates in multiple biologic functions such as gene transcription, cell cycle, DNA damage repair, and innate immunity and is implicated in

tumorigenesis by affecting metastasis, therapy resistance, and immune resistance [15]. SUMOylation refers to the covalent attachment of the small ubiquitin-like modifier (SUMO) family of proteins to lysine residues in specific target proteins through an enzymatic cascade [16]. Our further bioinformatics analyses identified SUMO1 as a gene inversely correlated with VWC2. SUMO1 has been recently observed as an oncogene in human cancers by stabilizing the protein of cancer driver genes via the SUMOylation modification [17, 18]. Moreover, the SUMO1 has been found to modify DNMTs [19]. Taken together, we postulated that the SUMO1 possibly affects the protein stability of certain DNMTs to govern the DNA methylation level of VWC2 in CRC.

Patients and methods

Patients. Eighty-six patients with CRC treated at the Second Hospital of Anhui Medical University from January 2018 to January 2020 were included in this research. The tumor and para-tumorous tissue samples were stored at -80°C . All malignant or benign samples were confirmed by hematoxylin and eosin staining before usage. None of the included patients received chemo- or radiotherapies before sample collection, and they all provided a written informed consent form. This research was ratified by the Ethics Committee of the Second Hospital of Anhui Medical University and abided by the Declaration of Helsinki.

Cells. Two CRC cell lines HCT-116 and HT29 were acquired from the American Type Culture Collection (Manassas, VA, USA). A human normal colon epithelial cell line NCM460 was acquired from BLUEFBIO Technology Co., Ltd. (Shanghai, China). All cells were maintained in Dulbecco's modified Eagle's medium (Thermo Fisher Scientific, Rockford, IL, USA) supplemented with 10% fetal bovine serum (FBS) and 100 units/ml penicillin/streptomycin (all from Thermo Fisher Scientific) at 37°C with 5% CO_2 .

A SUMOylation modification inhibitor COH000 (Cat No: S0309) and a protein synthesis inhibitor cycloheximide (Cat No: S7418) were procured from Selleck Chemicals (Houston, TX, USA). The COH000 was used to treat CRC cells at a dose of $0.2\ \mu\text{M}$ (IC50 of the *in vitro* SUMOylation), and cycloheximide was used at a dose of $100\ \mu\text{g}/\text{ml}$. Decitabine (HY-A0004, MedChemExpress, Monmouth Junction, NJ, USA) was used at $5\ \mu\text{M}$ to suppress the activity of DNMTs.

Plasmids and cell transfection. The routine overexpression vector pEX-4 (pGCMV/MCS/T2A/EGFP/Neo)-based overexpression plasmids of VWC2 (VWC2-OE), DNMT1 (DNMT1-OE), and the negative control (NC)-OE were procured from GenePharma Co., Ltd. (Shanghai, China). Mammalian shRNA-interference vector piggyBac (EGFP:T2A:Puro-U6)-based short hairpin RNAs (shRNAs) were procured from VectorBuilder Inc. (Guangzhou, Guangdong, China). The sequence information is listed below: sh-SUMO1 1#: 5'-TAAATAAGATCGACCAATGCAAGTGTTCATAATGACTTTCC-3'; sh-SUMO1

2#: 5'-GGAAAAATGACCTTTCCTTAACTTGAAGCTACTTTTAAAAT-3'; and sh-SUMO1 3#: 5'-ACAGGGTGTTC CAATGAATTC ACTCAGGTTTCTCTTTGAGG-3'. All plasmids were transfected to cells using Lipofectamine 2000 (Thermo Fisher Scientific) according to the instructions. At 48 h after transfection, the cells were harvested for subsequent analyses.

Reverse transcription-quantitative polymerase chain reaction (RT-qPCR). A TRIzol kit (Thermo Fisher Scientific) was used to isolate total RNA from tissues or cells. The RNA concentration was examined by NanoDrop 2000 spectrophotometer (Thermo Fisher Scientific), and the reverse transcription of RNA (100 ng) to cDNA was conducted by the iScript cDNA kit (Bio-Rad, Inc., Hercules, CA, USA). Real-time qPCR was performed by SYBRTM Green qPCR Master Mix (Thermo Fisher Scientific) on the 7900HT system (Thermo Fisher Scientific). Fold change of gene expression relative to GAPDH was determined by the $2^{-\Delta\Delta\text{Ct}}$ method. The PCR primers were designed and synthesized by Sangon Biotech Co., Ltd. (Shanghai, China), and the sequence information is listed below: VWC2 (Forward): 5'-GTGCCTGCTTGGGCTAGTTA-3'; VWC2 (Reverse): 5'-GGGGATGAGTGGGACTACCT-3'; SUMO1 (Forward): 5'-TCAACTGAGGACTTGGGGGA-3'; SUMO1 (Reverse): 5'-TCAGCAATTCTCTGACCCTCA-3'; GAPDH (Forward): 5'-AATGGGCAGCCGTTAGGAAA-3'; GAPDH (Reverse): 5'-GCGCCCAATACGACCAATC-3'.

Methylated DNA immunoprecipitation (MeDIP). Genomic DNA from cells was extracted using a DNA extraction kit (Thermo Fisher Scientific) and truncated to 200–600 bp DNA fragments by ultrasonication. According to the instructions of the MeDIP kit (BersinBio Co., Ltd., Guangzhou, Guangdong, China), highly-methylated DNA fragments were enriched by the 5mC antibody relative, followed by washing, elution, purification, and qPCR analysis. The percentage of DNA fragments enriched by the 5mC antibody to Input was calculated as the methylation level.

Western blot (WB) analysis. The cells were lysed in protease inhibitor-contained lysis buffer (Thermo Fisher Scientific) to isolate total protein, and the protein concentration was examined by a BCA kit (Thermo Fisher Scientific). Thereafter, an equal amount of protein sample ($50\ \mu\text{g}$) was separated by 10% SDS-PAGE and loaded onto polyvinylidene fluoride membranes (Sigma-Aldrich, Merck KGaA, Darmstadt, Germany). The membranes were blocked with 5% skim milk and hybridized with the primary antibodies overnight at 4°C , and then with HRP-labeled goat anti-rabbit IgG (1:3000, ab6721, Abcam) for 1 h. The signals were developed by enhanced chemiluminescence. The primary antibodies are listed below: anti-VWC2 (PA5-63097, Thermo Fisher Scientific), anti-SUMO1 (#4930, Cell Signaling Technology (CST), Beverly, MA, USA), anti-DNMT1 (1:1000, TU325877, Abmart Inc., Shanghai, China), and anti-GAPDH (internal control) (1:5000, TU363314, Abmart).

Co-immunoprecipitation (Co-IP). According to the instructions of the Co-IP kit (Thermo Fisher Scientific), the cells were lysed in a lysis buffer. A portion of the lysates was used as the Input for WB analysis, and another portion was incubated with anti-SUMO1 (#4940, CST) at 4°C overnight. After that, the protein A agarose beads were washed with lysis buffer and added to the cell lysates at 4°C for 2–4 h. The magnetic bead-protein complexes were collected and washed, and the protein sample was separated by SDS-PAGE and detected by WB analysis.

Chromatin immunoprecipitation (ChIP)-qPCR. Enrichment of VWC2 promoter by DNMTs was analyzed by the Pierce™ agarose ChIP kit (Thermo Fisher Scientific). In short, the CRC cells were soaked in formaldehyde for cross-linking. Later, the cells were lysed, and the chromatin was disrupted by ultrasonication. After that, the lysates were incubated with anti-DNMT1 (ab19905, Abcam), anti-DNMT3a (ab228691, Abcam), and DNMT3b (ab227883, Abcam) (all diluted at 1:200) overnight at 4°C, with rabbit IgG used as the control. The protein-DNA complexes were captured using the ChIP grade protein A/G Plus agarose, eluted, and then de-crosslinked. The purified DNA was collected for qPCR analysis to analyze the enrichment of VWC2 promoter fragments. The primer sequence information is listed below: Forward primer: 5'-CCAAGAT-GAAAGGTCCAGCG-3'; Reverse primer: 5'-GTTCC-GCTCCCTCCTCTG-3'.

Cell counting kit-8 (CCK-8) method. The cells were seeded in 96-well plates (1,000 cells per well) with a fresh culture medium. At 0, 12, 24, 36, 48, 72, and 96 h, respectively, 10 µl CCK-8 reagent (Sigma-Aldrich) was added to each well, followed by 4 h of incubation at 37°C. The optical density (OD) value was read by a microplate reader (Bio-Rad) at 450 nm to examine the cell viability.

Colony formation assay. Transfected CRC cells were seeded in six-well plates at 1,000 cells/well and routinely cultured for 2 weeks. Later, the cells were fixed by formaldehyde and stained with 0.1% crystal violet. The number of colonies (over 50 cells) was counted under the microscope.

Transwell assay. Transwell chambers (Unique Biotechnology Co., Ltd., Beijing, China) with 8 µm polycarbonate membrane filter were used to analyze the mobility of cells. For invasion detection, 2×10^4 cells were resuspended in a serum-free medium and loaded into apical chambers pre-coated with Matrigel (Unique). The basolateral wells were filled with 10% FBS complete medium. After 24 h of incubation at 37°C with 5% CO₂, cells that invaded the lower chambers were fixed and stained with crystal violet. The number was calculated under the microscope. Migration of cells was performed via similar procedures with the exception of Matrigel pre-coating on the apical chambers.

Xenograft tumors. HT29 cells stably infected with lentivirus (LV)-carried shRNAs (pLV-EGFP:T2A:Puro-U6 vector; VectorBuilder Inc.) were used for *in vivo* experiments. The shRNA sequences are as follows: LV-shSUMO1:

5'-TAAATAAGATCGACCAATGCAAGTGTTTCATA-ATGACTTTCC-3'; LV-shDNMT1: 5'-GCAGTACCTG-GACGACCCTGACCTCAAATATGGGCAGCACC-3'; LV-shVWC2: 5'-CGAGTTCGGGGCAAGACCTATCAG-ACTTTGGAGGAGTTCG-3'.

BALB/c nude mice (6 weeks old, 20 g) were procured from Vital River Laboratory Animal Technology Co., Ltd. (Beijing, China). The mice were randomly allocated into 5 groups: LV-NC, LV-shSUMO1, LV-shDNMT1, LV-shSUMO1+LV-shVWC2, and LV-shDNMT1+LV-shVWC2 groups, n=5 in each. All mice were maintained in a constant condition at 25°C with 45% humidity and allowed free access to feed and water. Stably infected HT29 cells were resuspended to 1×10^7 cells/ml, and 20 µl cell suspension was injected into the nude mice at the armpit site. The growth condition of tumors was recorded every 7 d, and the tumor volume (V) was calculated as follows: $V = (a \times b^2)/2$, where “a” refers to the length and “b” the width. After 28 d, the mice were sacrificed with 1% pentobarbital sodium (150 mg/kg), and the tumor was collected and weighed. All animal experiments were ratified by the Animal Ethics Committee of the Second Hospital of Anhui Medical University and performed following the Guide for the Care and Use of Laboratory Animals (NIH). Great efforts were made to reduce the suffering of animals.

Immunohistochemistry (IHC). Tissue sections were incubated at 60°C for 2 h, dewaxed, rehydrated in ethanol, blocked with 3% H₂O₂ for 10 min, soaked in 0.01 M citric acid buffer at 98°C for 15 min, and cooled down at room temperature. After that, the tissues were washed, incubated with normal serum for 30 min, and reacted with anti-VWC2 (PA5-63097, Thermo Fisher Scientific), anti-SUMO1 (1:200, #4930, CST), anti-DNMT1 (1:200, TU325877, Abmart), and anti-Ki-67 (1: 500, ab16667, Abcam) at 4°C overnight, and then with HRP-labeled goat anti-rabbit IgG (1:2000, ab6721, Abcam) at room temperature for 1 h. After that, the staining was developed with a DAB kit (#ZLI-9032, ZSGB-Bio Co., Ltd., Beijing, China), and the sections were viewed under the microscope (Leica Biosystems, Shanghai, China).

Statistical analysis. Data were analyzed by Prism 8.02 (GraphPad, La Jolla, CA, USA). Measurement data were expressed as the mean ± standard deviation (SD). For cellular experiments, at least three repetitions were performed. The t-test was used to analyze the difference between the two groups, and one- or two-way ANOVA was used to analyze the difference among multiple groups. Clinical parameters of patients were analyzed by Fisher's exact test. A p-value <0.05 was set to the threshold value for statistical significance.

Results

VWC2 has a DNA hypermethylation state in CRC. Aberrant DNA methylation is closely linked to the progression of CRC [20]. We queried the genes with DNA hypermethylation in colonic adenocarcinoma (COAD) via the UALCAN system, with VWC2 identified as the one with the

highest degree of DNA methylation (Figure 1A). Meanwhile, VWC2 also showed DNA hypermethylation in rectal adenocarcinoma (READ) (Figure 1B). In the MethSurv system (<https://biit.cs.ut.ee/methsurv/>), a higher DNA methylation level of VWC2 was linked to a lower survival rate of patients (Figure 1C). Moreover, we analyzed the DNA methylation of VWC2 in the collected tissue samples using MeDIP. The results showed that the DNA methylation level of VWC2 was markedly elevated in CRC tissues compared to the paratumorous tissues (Figure 1D). Similar results were observed *in vitro* where VWC showed increased DNA methylation levels in all CRC cells compared to the normal NCM460 cells (Figure 1E).

Low expression of VWC2 is linked to poor prognosis of patients. DNA hypermethylation in general leads to transcriptional suppression of genes. As expected, VWC2 showed a low-expression profile in CRC in the UALCAN system (Figure 2A). In the Kaplan-Meier Plotter system (<http://kmplot.com/analysis/index.php?p=service>), reduced expression of VWC2 is suggested to be linked to the low survival rate of patients (Figure 2B).

The VWC2 expression in the collected tissue samples was analyzed thereafter, and significantly reduced VWC2 expression was detected in the CRC tissues versus the adjacent non-involved tissues (Figure 2C), which presented an inverse correlation with its DNA methylation level (Figure 2D). Likewise, reduced VWC2 expression was detected in the CRC cells as well (Figure 2E). Treatment with the DNA methylation inhibitor decitabine in these cells significantly reduced the DNA methylation level and restored the VWC2 expression (Figures 2F, 2G).

Based on the mean value of VWC2 expression in CRC tissues (0.272), the patients were divided into the high-VWC2 expression (n=43) and the low-VWC2 expression (n=43) groups. As shown in Table 1, reduced VWC2 expression was

linked to increased lymph node metastasis, advanced TNM stage, and increased concentrations of tumor markers (CEA and CA-199).

Restoration of VWC2 suppresses the malignant growth of CRC cells. To uncover the function of VWC2 in CRC, upregulation of VWC2 was induced in HCT-116 and HT29 cells through the administration of VWC2-OE. The restoration of VWC2 expression in cells was detected by RT-qPCR (Figure 3A). Under this condition, the proliferation (Figure 3B) and colony formation (Figure 3C) of the CRC cells were significantly blocked. Moreover, the VWC2 upregulation reduced the number of cancer cells that migrated to or invaded the basolateral Transwell chambers (Figures 3D, 3E). This evidence reveals the suppressive effect of VWC2 on the activity of CRC cells.

The SUMO1 modification maintains the protein stability of DNMT1. To explore the mechanism responsible for DNA hypermethylation and downregulation of VWC2 in CRC, we explored the genes with negative correlation in VWC2 in the UALCAN (Figure 4A). Among the candidate genes, SUMO1 has been reported to modify the stability of target proteins [17, 18]. Moreover, the SUMO1 has been found to modify DNMTs [19]. Considering that the VWC2 showed DNA hypermethylation, we postulated that SUMO1 possibly affects specific DNMTs to affect the methylation level of VWC2.

Data in the GEPIA system (<http://gepia.cancer-pku.cn/index.html>) suggested that SUMO1 is highly expressed in CRC (Figure 4B). Moreover, we obtained via the Kaplan-Meier Plotter system that high SUMO1 expression is linked to poor survival of patients (Figure 4C). We next focused on the enrichment of DNMTs in the VWC2 promoter in CRC cells. The ChIP-qPCR assay revealed that the DNMT1 had the highest enrichment level in the VWC2 promoter (Figure 4D). The subsequent Co-IP and WB assays showed that DNMT1 had significantly increased SUMO1 modification levels in CRC cells, and the protein levels of DNMT1 and SUMO1 were both elevated in the CRC cells (Figure 4E).

To examine the role of SUMO1 in CRC, the shRNAs of SUMO1 were transfected in the CRC cells. The WB assay showed that the suppression of SUMO1 expression also led to a decline in the protein expression of DNMT1 (Figure 4F). The sh-SUMO1# with the best inhibitory effect was selected for subsequent use. The Co-IP and WB assay showed that the SUMO1 downregulation reduced the SUMO1 modification of DNMT1 in cells (Figure 4G). Moreover, the sh-SUMO1-transfected CRC cells were treated with the SUMOylation inhibitor COH000 and a protein synthesis inhibitor CHX. It was observed that the inhibition of the SUMO1 modification significantly reduced the protein stability of DNMT1 (Figure 4H).

SUMO1-DNMT1-mediated DNA methylation of VWC2 affects the malignant phenotype of CRC cells. The CRC cells stably transfected with sh-SUMO1 were further transfected with the overexpression DNA plasmid of DNMT1.

Table 1. Correlation of VWC2 expression with the clinical parameters of patients with CRC.

Clinical parameters	Total cases (n=86)	VWC2 expression		p-value
		Low (n=43)	High (n=43)	
Sex	Male	49	22	0.3838
	Female	37	21	
Age	≥60	50	24	0.8272
	<60	36	19	
Lymph node metastasis	Positive	42	31	****<0.0001
	Negative	44	12	
CEA (ng/ml)	≥10	20	17	***0.0006
	<10	66	26	
CA-199 (U/ml)	≥20	18	14	*0.0155
	<20	68	29	
TNM stage	I-II	43	13	***0.0005
	III-IV	43	30	

Note: clinical parameters of patients were analyzed by Fisher's exact test; *p<0.05, ***p<0.001, ****p<0.0001

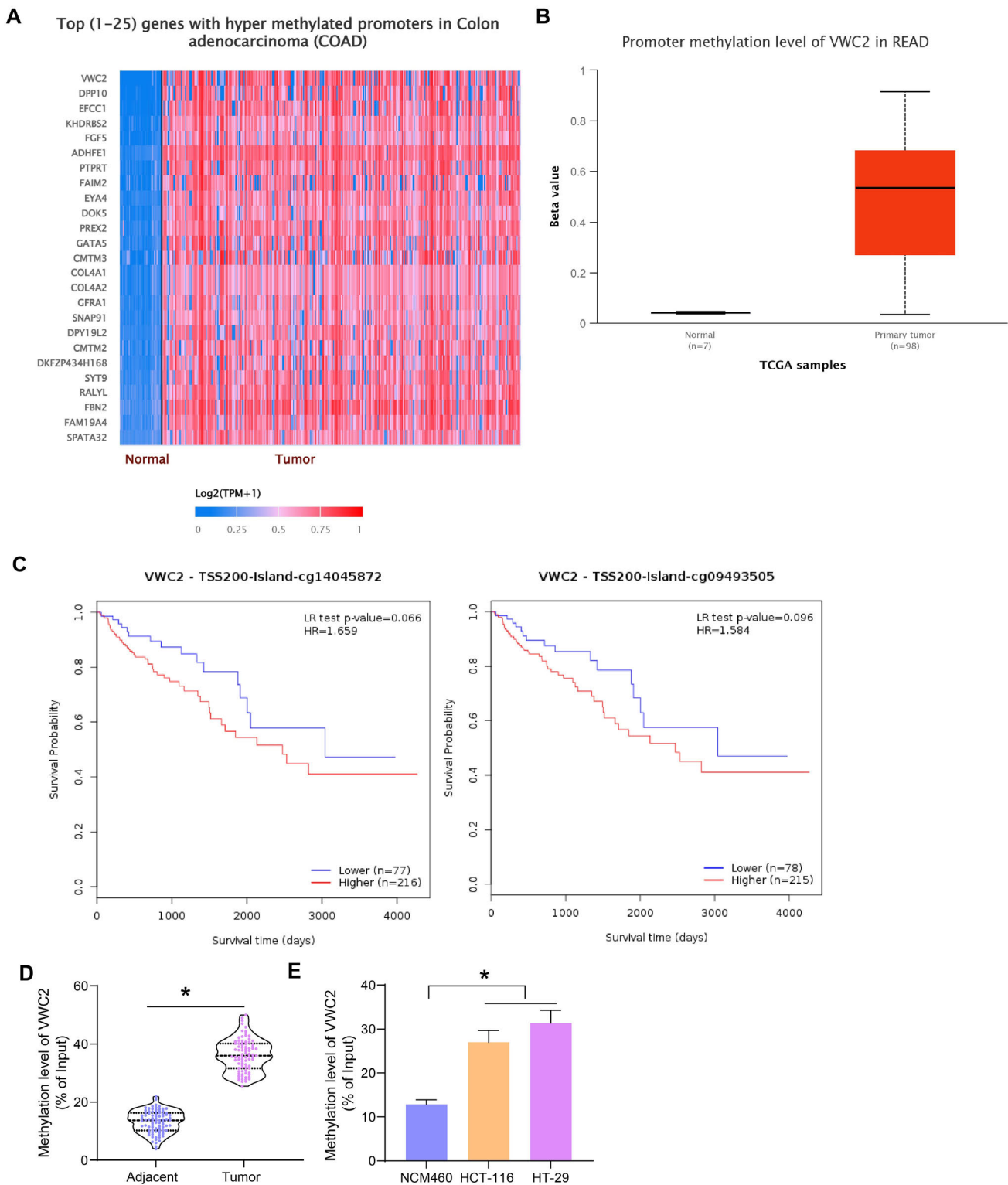


Figure 1. VWC2 has a DNA hypermethylation state in CRC. A) genes with DNA hypermethylation in COAD predicted in UALCAN; B) DNA methylation level of VWC2 in READ predicted in UALCAN; C) correlation of the VWC2 DNA methylation level with the survival rate of patients; D) VWC2 DNA methylation level in the collected CRC tissues and the adjacent tissues examined by MeDIP (n=86); E) VWC2 DNA methylation level in CRC cells and normal NCM460 cells detected by MeDIP. Differences were compared by the paired t-test (D) or one-way ANOVA (E). Three repetitions were performed. * $p < 0.05$

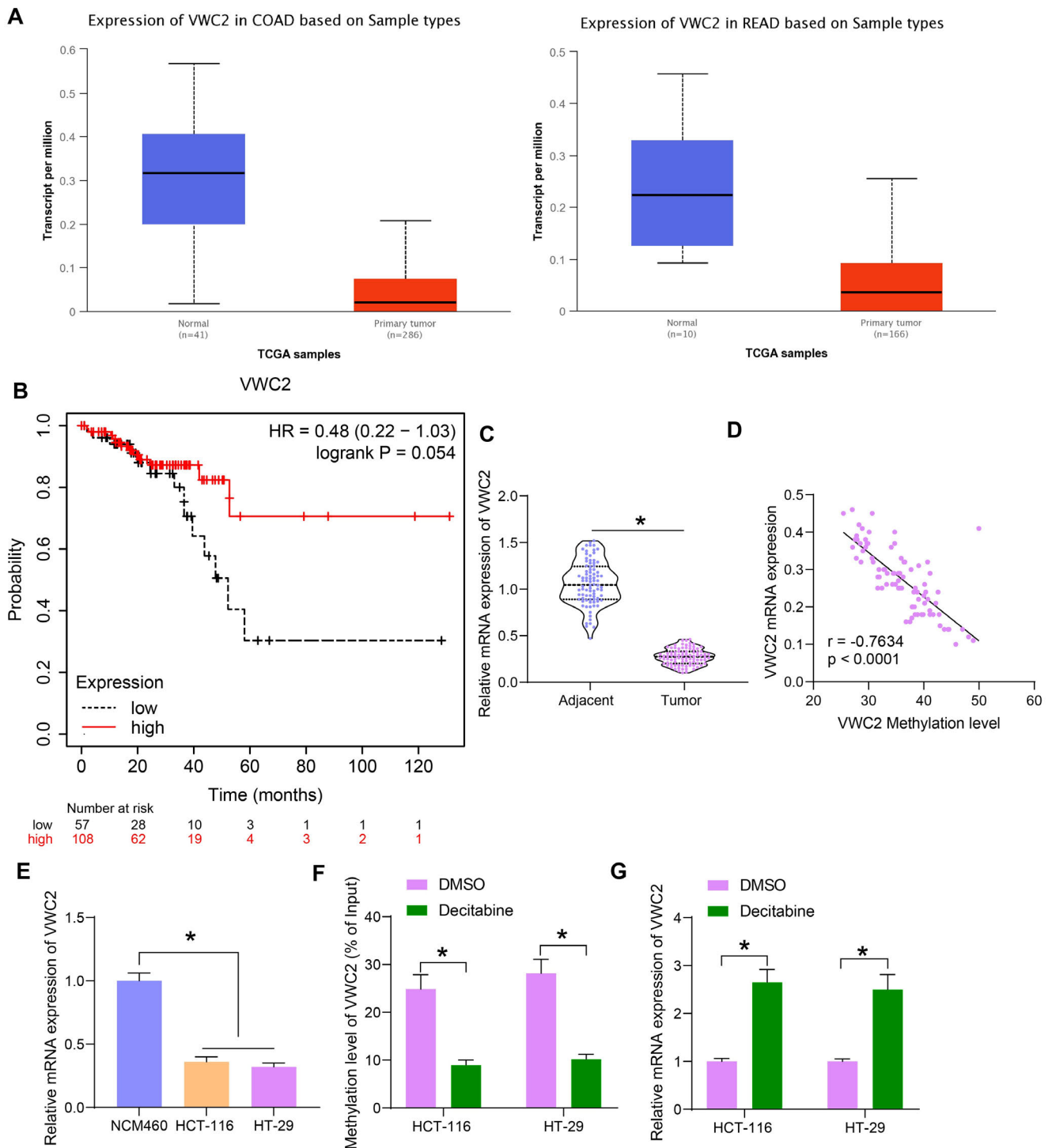


Figure 2. Low expression of VWC2 is linked to poor prognosis in patients. **A)** expression profile of VWC2 in CRC predicted in UALCAN; **B)** correlation of VWC2 expression with the CRC patient's survival analyzed in Kaplan-Meier Plotter; **C)** VWC2 expression in the collected CRC tissues and the adjacent tissues examined by RT-qPCR (n=86); **D)** correlation of VWC2 expression with the DNA methylation level in CRC tissues (n=86); **E)** VWC2 expression in CRC cells and normal NCM460 cells detected by RT-qPCR; **F)** VWC2 DNA methylation level in CRC cells after decitabine treatment determined by MeDIP; **G)** VWC2 expression in CRC cells after decitabine treatment determined by RT-qPCR. Correlation in panel D was analyzed by Pearson's correlation analysis. Differences were compared by the paired t-test (C), one-way ANOVA (E), or two-way ANOVA (F, G). Three repetitions were performed. *p<0.05

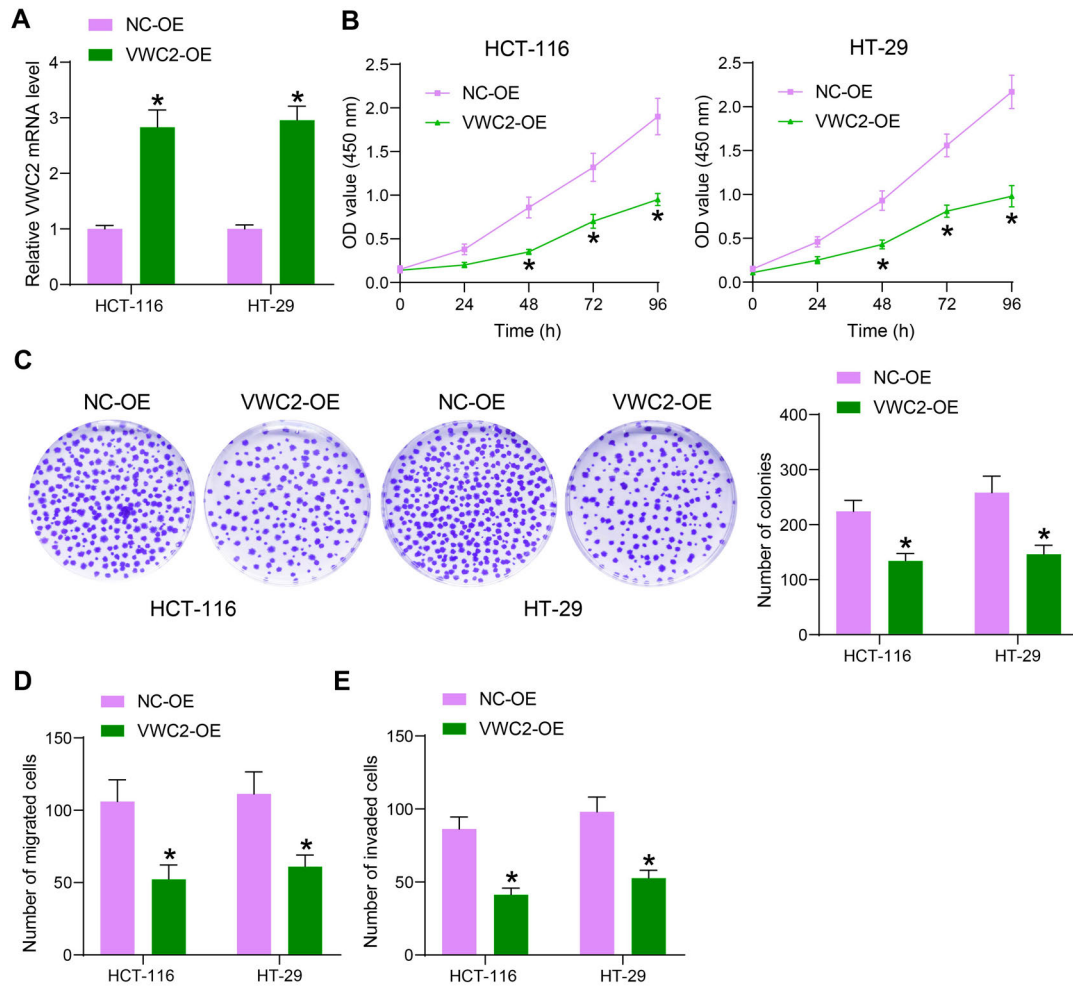


Figure 3. Restoration of VWC2 suppresses the malignant growth of CRC cells. A) upregulation efficiency of VWC2 in HCT-116 and HT29 cells examined by RT-qPCR; B) proliferation activity of the CRC cells examined by the CCK-8 assay; C) colony formation ability of cells analyzed by the colony formation assay; D, E) migration and invasion of CRC cells analyzed using the Transwell chambers. Differences were compared by the two-way ANOVA (A-E). Three repetitions were performed. * $p < 0.05$

The successful DNMT1 overexpression in cells was detected by WB analysis (Figure 5A). The MeDIP assay showed that the DNA methylation level of VWC2 was reduced by SUMO1 suppression but increased upon further DNMT1 overexpression (Figure 5B). Correspondingly, the transcription of VWC2 in cells was increased by SUMO1 suppression but suppressed by DNMT1 overexpression (Figure 5C).

Next, the CCK-8 and colony formation assays revealed that the proliferation and colony formation ability of the CRC cells was suppressed by sh-SUMO1 but restored by DNMT1-OE (Figures 5D, 5E). Moreover, the number of cells that migrated to or invaded the basolateral chambers in the Transwell assay was decreased by SUMO1 inhibition but restored by DNMT1 overexpression (Figure 5F, 5G).

Silencing of VWC2 restores xenograft tumor growth in nude mice suppressed by SUMO1 or DNMT1 knockdown. To further examine the SUMO1-DNMT1-VWC2 interac-

tion in CRC development, HT29 cells, which showed higher malignancy *in vitro*, were infected with LV-shSUMO1, LV-shDNMT1, and LV-shVWC2 and injected into mice to induce subcutaneous xenograft tumors.

Either LV-shSUMO1 or LV-shDNMT1 infection significantly suppressed the growth rate and weight of the xenograft tumors; however, the tumor growth in nude mice was significantly augmented upon the downregulation of VWC2 (Figures 6A, 6B). The tumor tissues were also collected for IHC assay, which showed that LV-shSUMO1 infection led to significantly decreased levels of SUMO1, DNMT1, and the proliferation marker Ki-67 in tissues but increased the VWC2 expression. Likewise, LV-shDNMT1 decreased the DNMT1 and Ki-67 levels but elevated the VWC2 expression. By contrast, the LV-shDNMT1 led to a decline in VWC2 expression and then the restoration of Ki-67 in the tumor tissues (Figures 6C–6F).

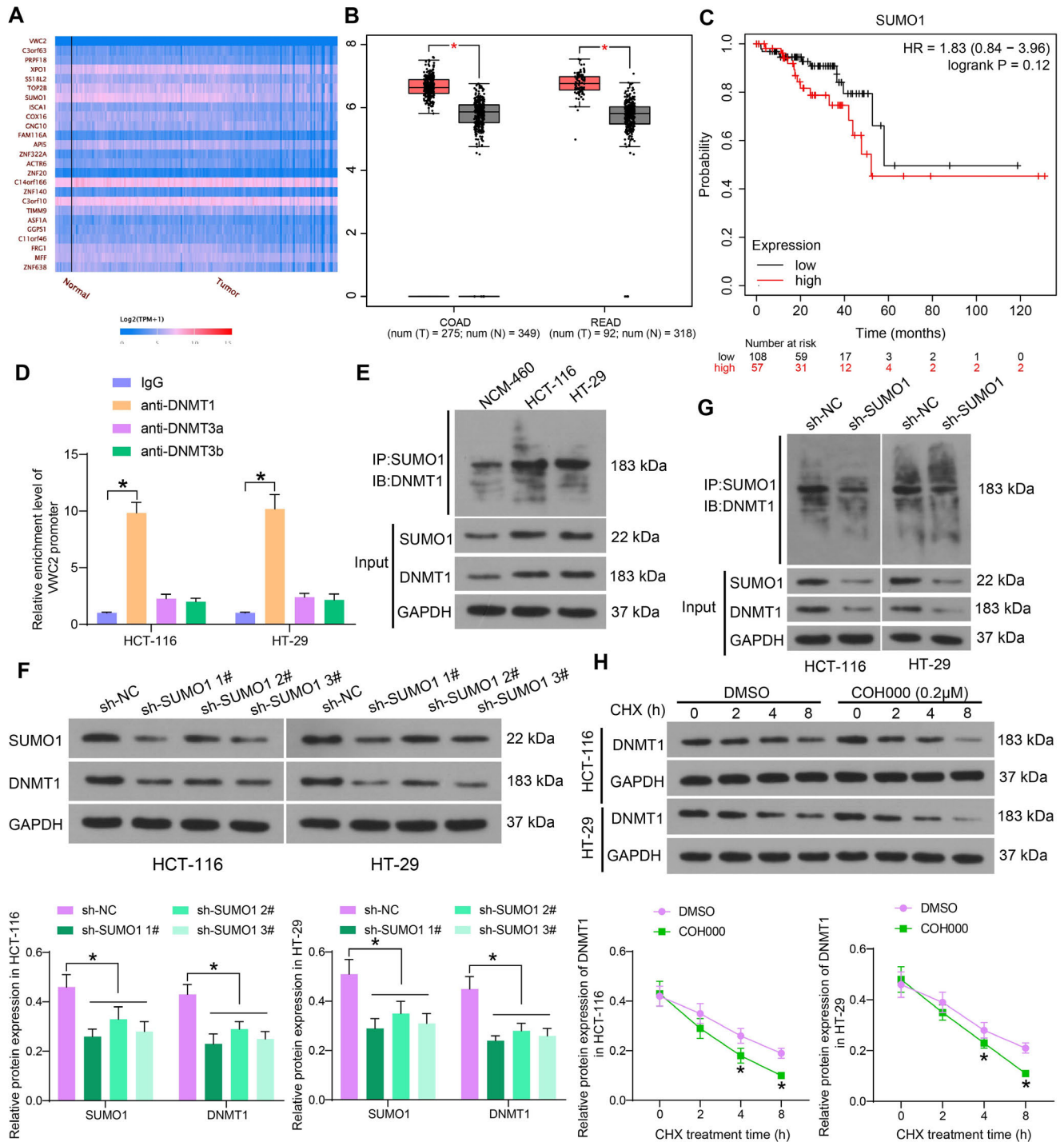


Figure 4. The SUMO1 modification maintains the protein stability of DNMT1. **A)** genes with negative correlation with WWC2 predicted in UALCAN; **B)** SUMO1 expression in CRC predicted in the GEPIA system; **C)** correlation of the SUMO1 expression with the survival of patients predicted in the Kaplan-Meier Plotter system; **D)** enrichment of WWC2 promoter fragments by DNMT1, DNMT3a, or DNMT3b analyzed by the ChIP-qPCR assay; **E)** SUMO1 and DNMT1 protein levels and the SUMO1 modification level of DNMT1 in CRC and the normal NCM460 cells analyzed by the Co-IP and WB assays; **F)** SUMO1 and DNMT1 protein levels in CRC cells after sh-SUMO1 transfection determined by WB analysis; **G)** SUMO1 modification level of DNMT1 in cells after sh-SUMO1 transfection determined by the Co-IP and WB assays; **H)** effect of the SUMO1 modification of DNMT1 on its protein stability. Differences were compared by the two-way ANOVA (D, F, H). Three repetitions were performed. * $p < 0.05$

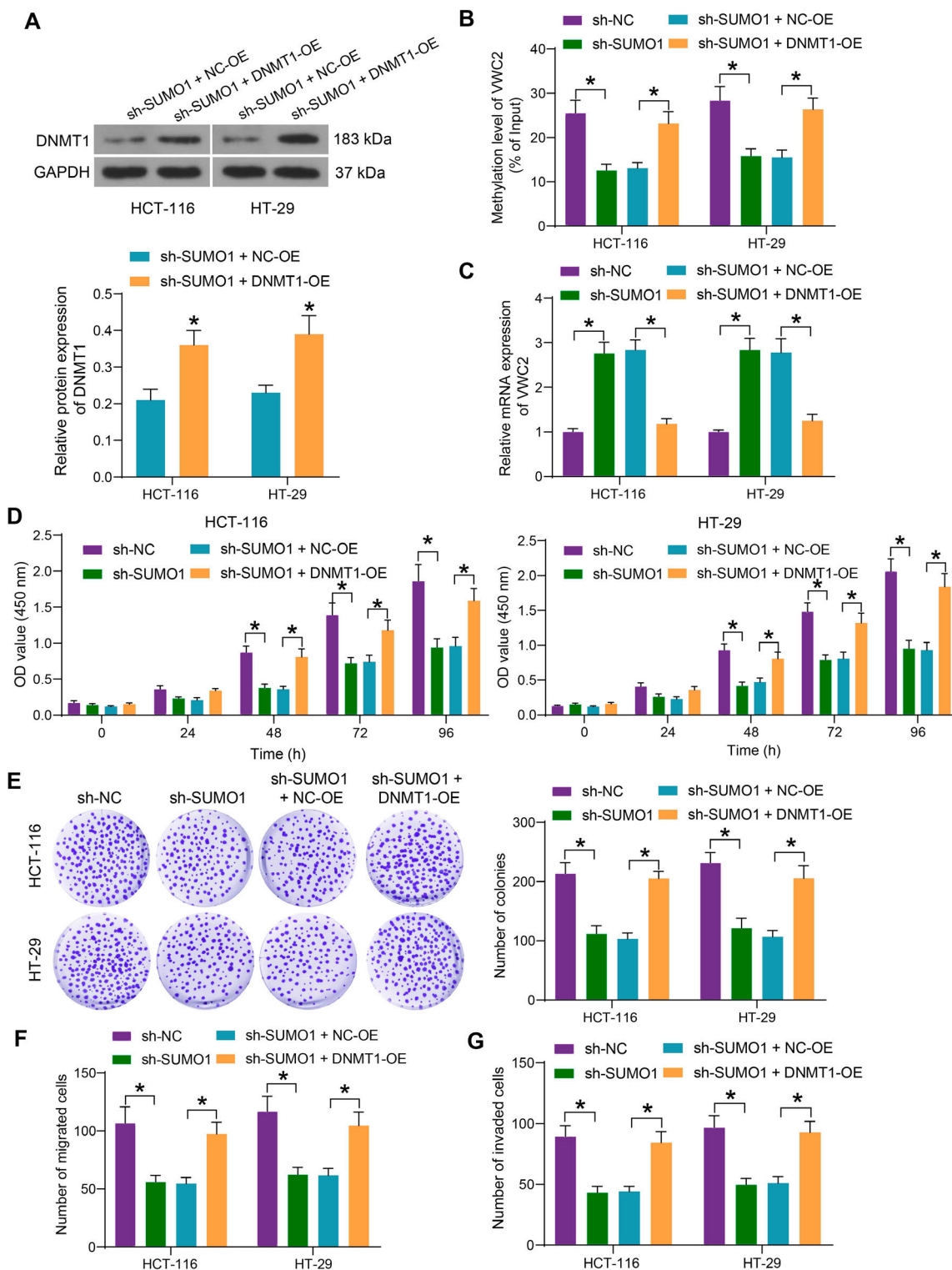


Figure 5. SUMO1-DNMT1-mediated DNA methylation of VWC2 affects the malignant phenotype of CRC cells. **A)** successful upregulation of DNMT1 in CRC cells by DNMT1-OE detected by WB analysis; **B)** VWC2 DNA methylation level in CRC cells after sh-SUMO1 and DNMT1-OE transfections determined by MeDIP; **C)** VWC2 mRNA expression in CRC cells after sh-SUMO1 and DNMT1-OE transfections determined by RT-qPCR; **D)** proliferation activity of the CRC cells examined by the CCK-8 assay; **E)** colony formation ability of cells analyzed by the colony formation assay; **F-G,** migration (**F**) and invasion (**G**) of CRC cells analyzed using the Transwell chambers. Differences were compared by the two-way ANOVA (**A-G**). Three repetitions were performed. * $p < 0.05$

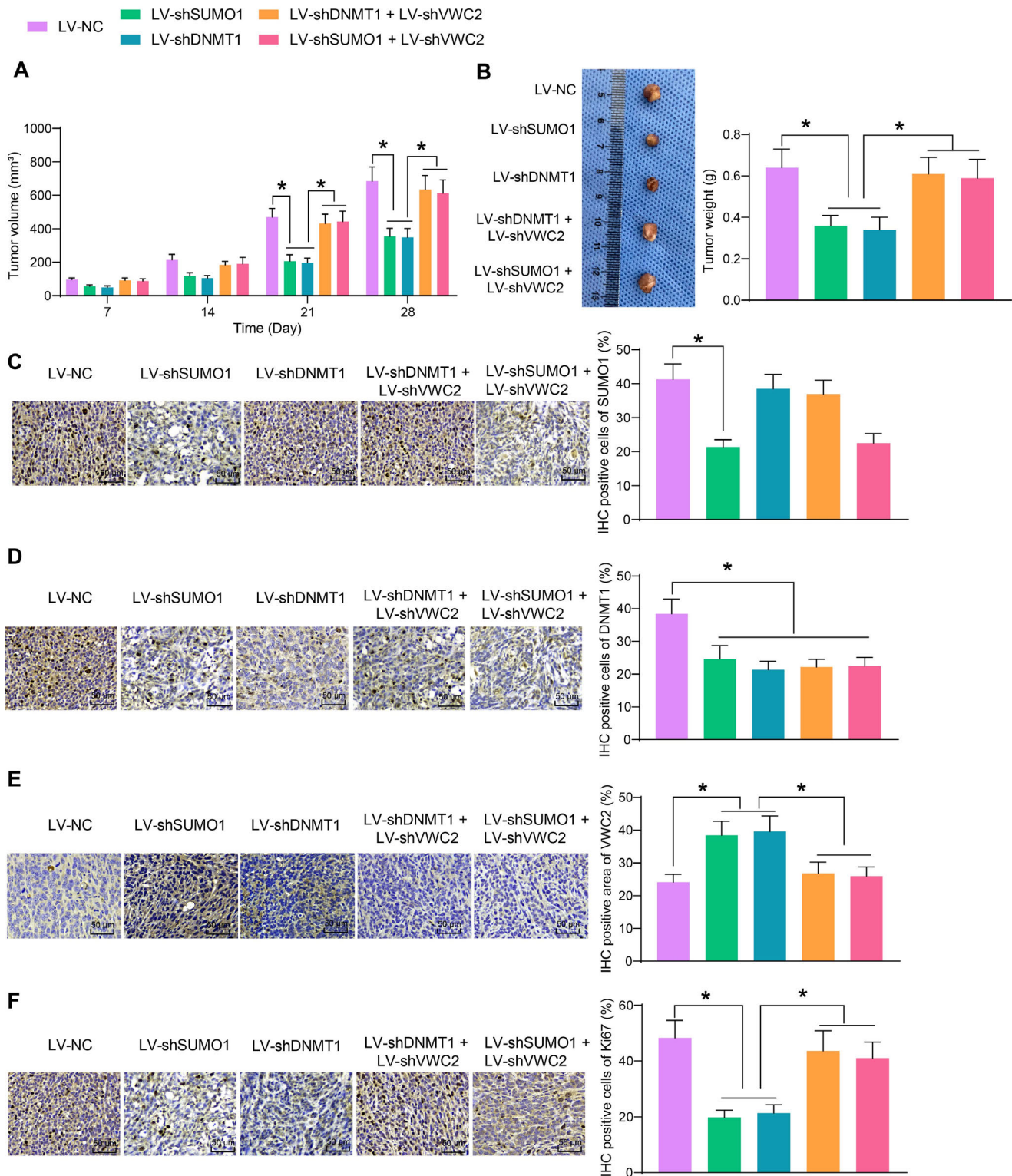


Figure 6. Silencing of VWC2 restores xenograft tumor growth in nude mice suppressed by SUMO1 or DNMT1 knockdown. A) volume change of the xenograft tumors in nude mice; B) weight of the xenograft tumors in nude mice; C-F) expression of SUMO1, DNMT1, VWC2, and Ki-67 in tumor tissues examined by IHC assay. In each group, n=5. Differences were analyzed by the one-way ANOVA (B-F) or two-way ANOVA (A). *p<0.05

Discussion

It is clear that recurrent tumor-specific DNA hypermethylation is closely linked to the onset and development of tumors, leaving DNA methylation as a promising diagnostic and prognostic marker as well as a therapeutic target for the control of cancers, including CRC [21–23]. In this work, we report that VWC2 functions as a tumor suppressor gene in CRC; however, it shows a low-expression pattern in tumors owing to the DNA hypermethylation induced by the SUMO1/DNMT1 axis.

We queried the genes with aberrant DNA methylation in CRC via the UALCAN system with VWC2 as the most promising candidate gene, and the VWC2 expression was predicted to be linked to poor prognosis of cancer patients. Later, DNA hypermethylation and decreased gene expression of VWC2 were detected in CRC cells. Although there has no evidence concerning the role of VWC2 in tumorigenesis, studies have provided clear evidence the DNA hypermethylation of specific genes is correlated with tumor progression. For instance, secreted frizzled related protein 1, an antagonist of the Wnt/ β -catenin pathway, was found to have increased DNA methylation in CRC, which leads to the Wnt/ β -catenin activation and increased stemness of cancer cells [24]. Similarly, hypermethylation of the tumor suppressor gene dual specificity tyrosine-phosphorylation-regulated kinase 2 augmented carcinogenesis in CRC [25]. DNA methylation-induced downregulation of Teashirt zinc finger homeobox 3 led to increased proliferation, resistance to apoptosis, and metastasis of CRC cells [26]. In this work, we first analyzed the clinical characteristics of patients and identified that poor VWC2 expression was linked to tumor metastasis and increased tumor marker expression. Moreover, we induced VWC2 overexpression in CRC cells. As a consequence, cell proliferation, colony formation, migration, and invasion

were significantly blocked. Therefore, we reported VWC2 as a tumor suppressor gene in CRC.

As for the mechanism responsible for DNA hypermethylation of VWC2 in CRC, we obtained SUMO1 as a gene showing a significant inverse correlation with VWC2 via the UALCAN system. SUMO1 represents a typical E3 SUMO protein ligase, that can be covalently conjugated to proteins as a single moiety [27]. The monomeric SUMO1 can interact with other proteins through the SUMO-interactive motif [28]. A previous report by Yang et al. revealed that SUMO1 modulates SUMOylation of MAF bZIP transcription factor B (MFAB) at lysine 32, therefore stabilizing MFAB protein to promote the growth of CRC cells *in vitro* and *in vivo* [29]. Likewise, SUMO1-mediated SUMOylation of IQGAP1 at lysine 1445 also leads to IQGAP1 stabilization and the tumorigenesis of CRC [30]. The oncogenic role of SUMO1 has also been reported in a recent publication by Liu et al. [31], and the oncogenic function may also involve the Wnt/ β -catenin signaling pathway [32]. In this work, to explore the potential correlation of SUMO1 and the aberrant DNA methylation of VWC2, we observed that the silencing of SUMO1 suppressed the SUMOylation of DNMT1, the most abundant DNMT enriched by the VWC2 promoter. Moreover, we found that SUMO1 bound to DNMT1 protein in the Co-IP assay. Therefore, we opine that the monomeric SUMO1 interacts with DNMT1 protein via the SUMO-interactive motif, therefore enhancing DNMT1 protein stability and consequently inducing VWC2 DNA methylation. DNMT1 has been demonstrated to function either as a tumor driver [33, 34] or a tumor suppressor [35, 36]. This discrepancy might be mainly attributable to the different downstream targets it affected. Here, our subsequent experiments revealed that the malignant behaviors of CRC cells *in vitro* were blocked upon SUMO1 silencing but restored after DNMT1 overexpression. Moreover, either silencing of SUMO1 or DNMT1

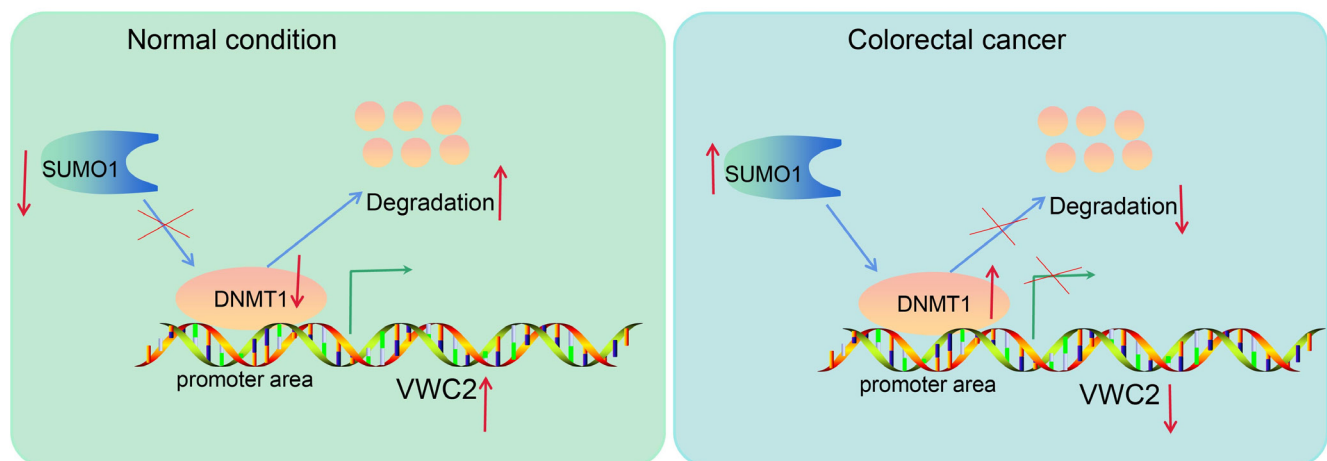


Figure 7. Graphical abstract. In CRC, highly expressed SUMO1 maintains protein stability of DNMT1 via SUMO1 modification, which subsequently catalyzes DNA methylation and transcriptional suppression of VWC2, leading to the malignant development of CRC.

suppressed the tumorigenic activity of CRC cells *in vivo*; however, the growth of xenograft tumors was restored upon further VWC2 silencing.

In conclusion, this study provides ample evidence that VWC2 plays an important tumor-suppressing role in CRC by blocking the proliferation and dissemination of CRC cells both *in vitro* and *in vivo*. The aberrant downregulation of VWC2 in cells was, at least partly, induced by the increased SUMO1 modification of DNMT1 (Figure 7). Therefore, SUMO1 or DNMT1 may serve as potential therapeutic targets while VWC2 as a therapeutic tool for CRC management. However, a major limitation of this study is that the downstream targets or pathways governed are not defined yet. We would like to investigate more molecules or signaling pathways regulated by VWC2 in future research.

Acknowledgments: This work was supported by the Natural Science Foundation for Youth (No. 2020xkj204).

References

- [1] ANDREI P, BATTUELLO P, GRASSO G, ROVERA E, TESIO N et al. Integrated approaches for precision oncology in colorectal cancer: The more you know, the better. *Semin Cancer Biol* 2022; 84: 199–213. <https://doi.org/10.1016/j.semcancer.2021.04.007>
- [2] SUNG H, FERLAY J, SIEGEL RL, LAVERSANNE M, SOERJOMATARAM I et al. Global Cancer Statistics 2020: GLOBOCAN Estimates of Incidence and Mortality Worldwide for 36 Cancers in 185 Countries. *CA Cancer J Clin* 2021; 71: 209–249. <https://doi.org/10.3322/caac.21660>
- [3] CHOU J, KALLER M, JAECKEL S, ROKAVEC M, HERMEKING H. AP4 suppresses DNA damage, chromosomal instability and senescence via inducing MDC1/Mediator of DNA damage Checkpoint 1 and repressing MIR22HG/miR-22-3p. *Mol Cancer* 2022; 21: 120. <https://doi.org/10.1186/s12943-022-01581-1>
- [4] MILLER KD, NOGUEIRA L, MARIOTTO AB, ROWLAND JH, YABROFF KR et al. Cancer treatment and survivorship statistics, 2019. *CA Cancer J Clin* 2019; 69: 363–385. <https://doi.org/10.3322/caac.21565>
- [5] SIEGEL RL, MILLER KD, GODING SAUER A, FEDEWA SA, BUTTERLY LF et al. Colorectal cancer statistics, 2020. *CA Cancer J Clin* 2020; 70: 145–164. <https://doi.org/10.3322/caac.21601>
- [6] BILLER LH, SCHRAG D. Diagnosis and Treatment of Metastatic Colorectal Cancer: A Review. *JAMA* 2021; 325: 669–685. <https://doi.org/10.1001/jama.2021.0106>
- [7] PORCELLINI E, LAPROVITERA N, RIEFOLO M, RAVAIOLI M, GARAJOVA I et al. Epigenetic and epitranscriptomic changes in colorectal cancer: Diagnostic, prognostic, and treatment implications. *Cancer Lett* 2018; 419: 84–95. <https://doi.org/10.1016/j.canlet.2018.01.049>
- [8] JONES PA. Functions of DNA methylation: islands, start sites, gene bodies and beyond. *Nat Rev Genet* 2012; 13: 484–492. <https://doi.org/10.1038/nrg3230>
- [9] PAN Y, LIU G, ZHOU F, SU B, LI Y. DNA methylation profiles in cancer diagnosis and therapeutics. *Clin Exp Med* 2018; 18: 1–14. <https://doi.org/10.1007/s10238-017-0467-0>
- [10] HATA T, DAL MOLIN M, HONG SM, TAMURA K, SUENAGA M et al. Predicting the Grade of Dysplasia of Pancreatic Cystic Neoplasms Using Cyst Fluid DNA Methylation Markers. *Clin Cancer Res* 2017; 23: 3935–3944. <https://doi.org/10.1158/1078-0432.CCR-16-2244>
- [11] HULBERT A, JUSUE-TORRES I, STARK A, CHEN C, RODGERS K et al. Early Detection of Lung Cancer Using DNA Promoter Hypermethylation in Plasma and Sputum. *Clin Cancer Res* 2017; 23: 1998–2005. <https://doi.org/10.1158/1078-0432.CCR-16-1371>
- [12] WU D, LI Y, REN Q, PEI S, WANG L et al. TANC1 methylation as a novel biomarker for the diagnosis of patients with anti-tuberculosis drug-induced liver injury. *Sci Rep* 2021; 11: 17423. <https://doi.org/10.1038/s41598-021-96869-5>
- [13] ALMEHMADI A, OHYAMA Y, KAKU M, ALAMOUDI A, HUSEIN D et al. VWC2 Increases Bone Formation Through Inhibiting Activin Signaling. *Calcif Tissue Int* 2018; 103: 663–674. <https://doi.org/10.1007/s00223-018-0462-9>
- [14] DAI X, ZHANG T, HUA D. Ubiquitination and SUMOylation: protein homeostasis control over cancer. *Epigenomics* 2022; 14: 43–58. <https://doi.org/10.2217/epi-2021-0371>
- [15] DU L, LIU W, ROSEN ST. Targeting SUMOylation in cancer. *Curr Opin Oncol* 2021; 33: 520–525. <https://doi.org/10.1097/CCO.0000000000000765>
- [16] WILKINSON KA, HENLEY JM. Mechanisms, regulation and consequences of protein SUMOylation. *Biochem J* 2010; 428: 133–145. <https://doi.org/10.1042/BJ20100158>
- [17] XU H, WANG H, ZHAO W, FU S, LI Y et al. SUMO1 modification of methyltransferase-like 3 promotes tumor progression via regulating Snail mRNA homeostasis in hepatocellular carcinoma. *Theranostics* 2020; 10: 5671–5686. <https://doi.org/10.7150/thno.42539>
- [18] ZHOU B, ZHU Y, XU W, ZHOU Q, TAN L et al. Hypoxia Stimulates SUMOylation-Dependent Stabilization of KDM5B. *Front Cell Dev Biol* 2021; 9: 741736. <https://doi.org/10.3389/fcell.2021.741736>
- [19] WANG H, SHEN YJ, LI XJ, XIA J, SUN L et al. DNMT3b SUMOylation Mediated MMP-2 Upregulation Contribute to Paclitaxel Induced Neuropathic Pain. *Neurochem Res* 2021; 46: 1214–1223. <https://doi.org/10.1007/s11064-021-03260-x>
- [20] GUTIERREZ A, DEMOND H, BREBI P, ILI CG. Novel Methylation Biomarkers for Colorectal Cancer Prognosis. *Biomolecules* 2021; 11: 1722. <https://doi.org/10.3390/biom11111722>
- [21] FOUAD MA, SALEM SE, HUSSEIN MM, ZEKRI ARN, HAFEZ HF et al. Impact of Global DNA Methylation in Treatment Outcome of Colorectal Cancer Patients. *Front Pharmacol* 2018; 9: 1173. <https://doi.org/10.3389/fphar.2018.01173>
- [22] JENSEN SO, OGAARD N, ORNTOFT MW, RASMUSSEN MH, BRAMSEN JB et al. Novel DNA methylation biomarkers show high sensitivity and specificity for blood-based detection of colorectal cancer—a clinical biomarker discovery and validation study. *Clin Epigenetics* 2019; 11: 158. <https://doi.org/10.1186/s13148-019-0757-3>

- [23] LAUGSAND EA, BRENNE SS, SKORPEN F. DNA methylation markers detected in blood, stool, urine, and tissue in colorectal cancer: a systematic review of paired samples. *Int J Colorectal Dis* 2021; 36: 239–251. <https://doi.org/10.1007/s00384-020-03757-x>
- [24] LI S, HAN Z, ZHAO N, ZHU B, ZHANG Q et al. Inhibition of DNMT suppresses the stemness of colorectal cancer cells through down-regulating Wnt signaling pathway. *Cell Signal* 2018; 47: 79–87. <https://doi.org/10.1016/j.cellsig.2018.03.014>
- [25] KUMAMOTO T, YAMADA K, YOSHIDA S, AOKI K, HIROOKA S et al. Impairment of DYRK2 by DNMT1-mediated transcription augments carcinogenesis in human colorectal cancer. *Int J Oncol* 2020; 56: 1529–1539. <https://doi.org/10.3892/ijo.2020.5020>
- [26] ZHOU Y, WANG S, YIN X, GAO G, WANG Q et al. TSHZ3 functions as a tumor suppressor by DNA methylation in colorectal cancer. *Clin Res Hepatol Gastroenterol* 2021; 45: 101725. <https://doi.org/10.1016/j.clinre.2021.101725>
- [27] QIN Y, LI Q, LIANG W, YAN R, TONG L et al. TRIM28 SUMOylates and stabilizes NLRP3 to facilitate inflammatory activation. *Nat Commun* 2021; 12: 4794. <https://doi.org/10.1038/s41467-021-25033-4>
- [28] CHANG HM, YE H. SUMO: From Bench to Bedside. *Physiol Rev* 2020; 100: 1599–619. <https://doi.org/10.1152/physrev.00025.2019>
- [29] YANG LS, ZHANG XJ, XIE YY, SUN XJ, ZHAO R et al. SUMOylated MAFB promotes colorectal cancer tumorigenesis. *Oncotarget* 2016; 7: 83488–83501. <https://doi.org/10.18632/oncotarget.13129>
- [30] LIANG Z, YANG Y, HE Y, YANG P, WANG X et al. SUMOylation of IQGAP1 promotes the development of colorectal cancer. *Cancer Lett* 2017; 411: 90–99. <https://doi.org/10.1016/j.canlet.2017.09.046>
- [31] LIU Q, HUANG Q, LIU H, HE FJ, LIU JH et al. SUMOylation of methyltransferase-like 3 facilitates colorectal cancer progression by promoting circ_0000677 in an m(6) A-dependent manner. *J Gastroenterol Hepatol* 2022; 37: 700–713. <https://doi.org/10.1111/jgh.15775>
- [32] WANG J, ZHANG Z, FANG A, WU K, CHEN X et al. Resveratrol Attenuates Inflammatory Bowel Disease in Mice by Regulating SUMO1. *Biol Pharm Bull* 2020; 43: 450–457. <https://doi.org/10.1248/bpb.b19-00786>
- [33] LUO Y, XIE C, BROCKER CN, FAN J, WU X et al. Intestinal PPARalpha Protects Against Colon Carcinogenesis via Regulation of Methyltransferases DNMT1 and PRMT6. *Gastroenterology* 2019; 157: 744–759 e4. <https://doi.org/10.1053/j.gastro.2019.05.057>
- [34] WANG C, MA X, ZHANG J, JIA X, HUANG M. DNMT1 maintains the methylation of miR-152-3p to regulate TMSB10 expression, thereby affecting the biological characteristics of colorectal cancer cells. *IUBMB Life* 2020; 72: 2432–2443. <https://doi.org/10.1002/iub.2366>
- [35] HAN J, CHEN X, XU J, CHU L, LI R et al. Simultaneous silencing Aurora-A and UHRF1 inhibits colorectal cancer cell growth through regulating expression of DNMT1 and STAT1. *Int J Med Sci* 2021; 18: 3437–3451. <https://doi.org/10.7150/ijms.61969>
- [36] LV L, HE L, CHEN S, YU Y, CHE G et al. Long Non-coding RNA LINC00114 Facilitates Colorectal Cancer Development Through EZH2/DNMT1-Induced miR-133b Suppression. *Front Oncol* 2019; 9: 1383. <https://doi.org/10.3389/fonc.2019.01383>